

Use of an artificial neural network model for estimation of unfrozen water content in frozen soils

Junping Ren¹, Xudong Fan², Xiong (Bill) Yu², Sai K Vanapalli³, and Shoulong Zhang⁴

¹Lanzhou University

²Case Western Reserve University

³University of Ottawa

⁴Hokkaido University

November 22, 2022

Abstract

A portion of pore water is typically in a state of unfrozen condition in frozen soils due to the complex soil-water interactions. The variation of the amount of unfrozen water and ice has a significant influence on the physical and mechanical behaviors of the frozen soils. Several empirical, semi-empirical, physical and theoretical models are available in the literature to estimate the unfrozen water content (UWC) in frozen soils. However, these models have limitations due to the complex interactions of various influencing factors that are not well understood or fully established. For this reason, in the present study, an artificial neural network (ANN) modeling framework is proposed and the PyTorch package is used for predicting the UWC in soils. For achieving this objective, extensive UWC data of various types of soils tested under various conditions were collected through an extensive search of the literature. The developed ANN model showed good performance for the test dataset. In addition, the model performance was compared with two traditional statistical models for UWC prediction on four additional types of soils and found to outperform these traditional models. Detailed discussions on the developed ANN model, and its strengths and limitations in comparison to different other models are provided. The study demonstrates that the proposed ANN model is simple yet reliable for estimating the UWC of various soils. In addition, the summarized UWC data and the proposed machine learning modeling framework are valuable for future studies related to frozen soils.

1

2 **Use of an artificial neural network model for estimation of**

3 **unfrozen water content in frozen soils**

4

5

6 Junping Ren¹, Xudong Fan^{2*}, Xiong (Bill) Yu², Sai K. Vanapalli³, Shoulong Zhang⁴

7

8 ¹ MOE Key Laboratory of Mechanics on Disaster and Environment in Western China, College

9 of Civil Engineering and Mechanics, Lanzhou University, Lanzhou 730000, China

10 ² Department of Civil and Environmental Engineering, Case Western Reserve University,

11 Cleveland 44106-7201, USA

12 ³ Department of Civil Engineering, University of Ottawa, Ottawa K1N6N5, Canada

13 ⁴ Division of Field Engineering for the Environment, Hokkaido University, Sapporo 060-8628,

14 Japan

15

16

17

18

19 *Corresponding author: Xudong Fan

20 Email: xxf121@case.edu

21

22

23

24 **Abstract**

25 A portion of pore water is typically in a state of unfrozen condition in frozen soils due to the
26 complex soil-water interactions. The variation of the amount of unfrozen water and ice has a
27 significant influence on the physical and mechanical behaviors of the frozen soils. Several
28 empirical, semi-empirical, physical and theoretical models are available in the literature to
29 estimate the unfrozen water content (UWC) in frozen soils. However, these models have
30 limitations due to the complex interactions of various influencing factors that are not well
31 understood or fully established. For this reason, in the present study, an artificial neural network
32 (ANN) modeling framework is proposed and the PyTorch package is used for predicting the
33 UWC in soils. For achieving this objective, extensive UWC data of various types of soils tested
34 under various conditions were collected through an extensive search of the literature. The
35 developed ANN model showed good performance for the test dataset. In addition, the model
36 performance was compared with two traditional statistical models for UWC prediction on four
37 additional types of soils and found to outperform these traditional models. Detailed discussions
38 on the developed ANN model, and its strengths and limitations in comparison to different other
39 models are provided. The study demonstrates that the proposed ANN model is simple yet
40 reliable for estimating the UWC of various soils. In addition, the summarized UWC data and
41 the proposed machine learning modeling framework are valuable for future studies related to
42 frozen soils.

43

44 **Keywords:** *Frozen soils, unfrozen water, artificial neural network, modeling framework,*
45 *prediction*

46

47

48

49 **1. Introduction**

50 The freezing of water to form ice is one of the most common phase transformations in the
51 natural environment (Wettlaufer, 1999). Nearly one-third of the land surface of the Earth
52 experiences freezing and thawing annually (Lu et al., 2021). In these permafrost and seasonally
53 frozen regions, unfrozen water and pore ice coexist within a frozen soil, due to the complex
54 soil-water interactions. The unfrozen water exists in small pore spaces by capillarity and as thin
55 films adsorbed on the surfaces of soil particles, in equilibrium with the pore ice at subzero
56 temperatures. The relationship between the amount of unfrozen water and its energy state in a
57 frozen soil is generally referred to as the soil-freezing characteristic curve (SFCC) in the
58 literature (Ren et al., 2021). The quantity of unfrozen water in the frozen soil can be represented
59 by either the gravimetric water content, or volumetric water content, or degree of unfrozen
60 water saturation. The energy state of unfrozen water is typically represented by the subzero
61 temperature of the frozen soil.

62 The SFCC links the degree of water-ice phase transition to the subzero temperature in a
63 frozen soil. Since the constitutive relationships for hydraulic, thermal, and mechanical fields of
64 frozen soils are functions of the quantity of unfrozen water, the SFCC is essential for modeling
65 the transport mechanism of water, heat, and solutes in frozen soils (e.g., Lai et al., 2014; Yu et
66 al., 2020a, b; Saberi and Meschke, 2021). For example, reliable determination of the unfrozen
67 water in frozen soils is valuable for predicting their hydraulic properties which are vital for
68 models of flood forecasting during spring thawing, and their mechanical properties that
69 determine the stability of the ground for infrastructure in cold regions (Amankwah et al., 2021).
70 In other words, a sound understanding of SFCC is critical for broad engineering applications
71 and for understanding the likely impacts associated with climate change (Lara et al., 2021).

72 Due to its essential role in cold regions science and engineering, an accurate description of
73 the unfrozen water content (UWC) is crucial to achieve a realistic representation of the behavior
74 of frozen soils. In addition, the increasing use of permafrost regions for civil infrastructure
75 constructions and the effects of global warming on these regions has further stimulated research
76 on the behavior of frozen soils (Shastri, 2014; Saberi and Meschke, 2021), among which the
77 UWC is a key property. Many models have been proposed to estimate the soil UWC or SFCC
78 during the last few decades. These proposed models are generally based on using soil physical

79 properties, the similarity between SFCC and soil-water characteristic curve (SWCC), and / or
80 physical and theoretical mechanisms (Ren, 2019). Amongst these models, the empirical models
81 were generally put forward by earlier researchers (e.g., Dillon and Andersland, 1966; Anderson
82 and Tice, 1972; Xu et al., 1985; Michalowski, 1993; Mckenzie et al., 2007). Most of the
83 empirical models are based on fitting experimental results, with a connection to the basic
84 physical properties of frozen soils (Ming et al., 2020) and subzero temperature. In recent years,
85 there has been significant interest in proposing physical, theoretical and thermodynamic models
86 for estimating UWC (e.g., Liu and Yu, 2013, 2014; Wang et al., 2017a; Amiri et al., 2018; Bai
87 et al., 2018; Chai et al., 2018; Mu et al., 2018; Teng et al., 2020; Zhou et al., 2020; Jin et al.,
88 2020; Xiao et al., 2020; Saberi and Meschke, 2021), that may be attributed to the better
89 understanding of physical mechanisms underlying the ice-water transition in porous media.
90 Some investigators have summarized these models in their research studies (e.g., Kurylyk and
91 Watanabe, 2013; Mu, 2017; Ren et al., 2017; Lu et al., 2019; Hu et al., 2020).

92 It is widely acknowledged that many factors influence the UWC in frozen soils. These
93 factors mainly include the soil physical and chemical properties, stress state, and temperature.
94 The complex effects of these factors result in a highly nonlinear relationship between these
95 factors and the UWC. In addition, the relative contribution of each factor on UWC is not well-
96 understood. This causes difficulties in selecting the most relevant factors for establishing a
97 reliable UWC model. Such difficulties can be effectively addressed by using machine learning
98 (ML) algorithms, such as the artificial neural network (ANN) models. The ANN is an adaptive
99 information-processing technique, which allows the correlations between input and output
100 variables to be established through inter-connected neurons (Saha et al., 2018). The key
101 advantage of an ANN model in comparison to empirical and statistical methods is that it does
102 not require any prior knowledge about the nature of the relationship between the input and
103 output variables (Shahin et al., 2001; Pham et al., 2019). In addition, it is able to take account
104 of various influencing factors that have weak or nonlinear relationships with the outcomes
105 (Zhang et al., 2021b; Zhong et al., 2021). For this reason, there is no need to either simplify the
106 problem or introduce simplified assumptions (Shahin et al., 2008). Moreover, ANN models can
107 always be updated to obtain better results by presenting new training examples as new data
108 become available (Ismeik and AI-Rawi, 2014; Zhong et al., 2021). These features make ANN

109 suitable for predicting soil behaviors affected by various factors.

110 The ANN has been widely employed in geotechnical and geo-environmental engineering
111 fields that include predicting soil stress–strain behavior (Habibagahi and Bamdad, 2003),
112 resilient modulus (Ren et al., 2019), and thermal conductivity / resistivity (e.g., Erzin et al.,
113 2008; Wen et al., 2020). Wang et al. (2020b) employed three ML models to estimate the UWC
114 of a frozen saline soil. Three influencing factors (i.e., temperature, sodium bicarbonate content,
115 and initial water content) were considered in their models. One limitation of their models,
116 however, is that the models were developed based on limited experimental data of a specific
117 soil. This largely restricts the use of their models for other applications. For this reason, in the
118 present study, UWC data of various types of soils tested under various conditions are collected,
119 through an extensive literature search. An ANN model is developed for estimating the UWC in
120 frozen soils, based on the collected large amount of experimental data. A modelling framework
121 is proposed and followed, and the ANN model is built by PyTorch package (Paszke et al., 2017).
122 The developed ANN model is further compared with two traditional statistical models for UWC
123 prediction. Detailed discussions on the developed ANN model and model comparison are also
124 presented. The present study is one of the earliest attempts to modeling UWC in frozen soils by
125 ML algorithms. It can provide good reference (e.g., collected data, modeling framework, and
126 programming scripts) for future studies related to the UWC prediction, and may be incorporated
127 in numerical codes for solving the coupled thermal–hydraulic–mechanical–chemical process in
128 frozen soils.

129

130 **2. Modeling framework and data sources**

131 Figure 1 represents the proposed framework for the prediction of UWC in frozen soils. The
132 main framework can be divided into data preparation (left part of Fig. 1), model optimization
133 (middle part of Fig. 1), and model application (right part of Fig. 1). The collected datasets are
134 prepared as a tabular dataset where the final column is the prediction target (i.e., volumetric
135 UWC). The first four columns of the prepared dataset are the specific surface area, dry density,
136 initial volumetric water content and temperature, respectively. With the prepared dataset, the
137 features' values are firstly normalized by scaling each factor into a distribution with zero mean
138 value and unit variance. This process is conducted to mitigate computational burden during the

139 model optimization and application processes, as well as to increase the model performance. In
140 the model optimization process, at each iteration, the normalized dataset will be randomly
141 divided into 80%:20%. The 80% samples are used to train the ANN model with given
142 hyperparameters, and the rest 20% samples are used for independent evaluation of the trained
143 model. Based on the evaluation results, Bayesian optimization algorithm is used to find the
144 optimal hyperparameters of the ANN model with better performance. The Bayesian
145 optimization process is iterated 50 times in the present study. After obtaining the optimal
146 hyperparameters, the ANN model is evaluated again with the k-folder cross validation. The
147 folder with best performance is used for Shapley Additive exPlanations (SHAP) interpretation
148 to determine the influence of considered factors on the prediction target.

149 The details about data collection, ANN model, Bayesian optimization, and k-folder cross
150 validation are discussed in the following sections from Section 2.1 to 2.4.

151

152 **2.1 Data collection**

153 In the present study, soil physical properties and the UWC data were obtained from the
154 literature. For the UWC, only data points which can be clearly identified (e.g., scattered data
155 points in figures or tabular data) were included. Those with only unfrozen water content curves
156 shown were not considered since it is not possible to identify the real measured UWC data
157 points. This avoids obtaining arbitrary data from the continuous UWC curves. The raw data
158 points were extracted from the original plots using GetData Graph Digitizer.

159 Factors that influence the UWC of frozen soils can be categorized into the internal and
160 external factors. The internal factors are typical soil physical properties, such as the particle size
161 distribution (PSD), sand/silt/clay content, plasticity indices, specific surface area (SSA), dry
162 density, void ratio (or porosity), initial water content and salinity. The external factors can
163 include temperature, stress state, freeze-thaw and wet-dry cycles, etc. The influencing factors
164 that were considered in various studies in the literature are different and sometimes arbitrary.
165 For example, [Smith and Tice \(1988\)](#), in their study considered four factors that include three
166 internal factors (SSA, initial water content and dry density) and one external factor
167 (temperature). In another study, [Kruse and Darrow \(2017\)](#) considered more factors such as soil
168 cation exchange capacity and cation treatment. Besides temperature, which typically has the

169 most significant effect on UWC, only a few studies considered other external factors such as
170 freeze-thaw cycles and stress state (e.g., [Mu, 2017](#); [Ren and Vanapalli, 2020](#)). Therefore, it is
171 difficult to find abundant data or studies that took into account exact the same types of
172 influencing factors. As a result, a search of more than 100 articles from the literature resulted
173 in identifying 20 articles that can be used in the present study, as listed in [Table 1](#).

174 In this study, the following factors were selected: SSA, dry density (ρ_d), initial volumetric
175 water content (θ_{init}) and temperature ($Temp$). This is because these four factors were considered
176 in all the 20 articles and the UWC data of a variety of soils are available (73 soils in [Table 1](#)).
177 It should be noted that the soil specimens used for UWC measurement were not necessarily
178 initially saturated. [Table 1](#) also indicates that the UWC data were mostly measured by nuclear
179 magnetic resonance (NMR) and time domain reflectometry (TDR), while some of them were
180 measured by other methods such as frequency domain reflectometry (FDR), time domain
181 transmissometry (TDT), etc. In order to increase the database, the UWC data was collected
182 regardless of the testing methods. The gravimetric water content was converted to volumetric
183 water content by multiplying by soil dry density. The thawing or freezing SFCC branch was
184 generally measured in the selected studies, while several studies measured both the thawing and
185 freezing branches. In addition, the supercooling portion on the freezing branch was abandoned
186 when collecting UWC data, since it does not represent a real unfrozen water portion.

187 Special attention was paid to the SSA which is not available for a few soils. In this case,
188 the SSA of these soils were either estimated or assumed in the present study. Several estimation
189 methods have been proposed in the literature. For example, [Ismeik and AI-Rawi \(2014\)](#)
190 suggested using equivalent diameter from the PSD to estimate SSA. [Ersahin et al. \(2006\)](#)
191 highlighted that fractal dimensions for PSD can be used as an integrating index in estimating
192 SSA. However, the soils collected in the present study do not necessarily have a PSD
193 information, making these two methods not applicable. On the other hand, according to
194 [Yukselen-Aksoy and Kaya \(2010\)](#), there is high correlation between the soil SSA and its liquid
195 limit or plasticity index. As soil consistency limit values are generally available, the SSA of
196 several soils was estimated by the relationship between SSA and plasticity index, suggested by
197 [Yukselen-Aksoy and Kaya \(2010\)](#) (Eq. (7) in their study). However, for those soils that do not
198 have a plasticity index, such as sand, their SSA were assumed according to typical values for

199 those types of soils.

200

201 **2.2 Artificial neural network model**

202 The ANN is one of the supervised ML models (Fan et al., 2021). Figure 2 shows a typical
203 structural ANN model that contains one input layer, three hidden layers and one output layer.
204 In the input layer, the number of neurons equals the number of input variables. The number of
205 neurons in the hidden layers determines the nonlinear degree of the designed model. In the
206 present study, only one neuron is used in the output layer as a regression model, which
207 represents the predicted volumetric UWC. For each neuron in the ANN, the output vector can
208 be determined by Eq. (1) (Dongare et al., 2012),

$$209 \quad y_k = f\left(\sum_{r=1}^I \omega_{r,k} x_r\right) \quad (1)$$

210 where, y_k is the output of neuron k ; x_r is the input values from neurons of previous layer; $\omega_{r,k}$ is
211 the weight of each input value. The weight will be optimized in the forward and backward
212 propagation process. $f(\bullet)$ is the activation function used to increase the nonlinear property
213 during the propagation. In the present study, the ‘ReLU’ function is used as the activation
214 function for the hidden layers and the ‘Linear’ activation function is used for the output layer.

215 As can be seen from the architecture of ANN model, comparing to traditional statistical
216 models, the advantage of using ANN model is that the model releases the fixed mathematical
217 equation by combining the linear equation and activation function at each neuron. Therefore,
218 no prior knowledge is required to predefine the relationship between the input variables and
219 prediction target.

220

221 **2.3 Bayesian optimization**

222 The ANN model does not need any predefined relationship between the input and output
223 variables; however, the final performance is heavily influenced by the architecture of the ANN
224 model. A few hyperparameters inside the ANN model may influence its final prediction
225 performance, such as the batch size, number of hidden layers, number of neurons in each layer,
226 the type of optimizer and corresponding learning rate. In the present study, a Bayesian
227 optimization method is used for tuning these hyperparameters to maximize the model’s

228 performance.

229 The Bayesian optimization used in this study is adopted from the scikit-optimization
230 package (Head et al., 2018). In particular, the Bayesian optimization process aims to solve the
231 optimization problem as shown in Eq. (2). As the target function $f(x)$ represents the loss value
232 of ANN model that cannot get the gradient directly, a surrogate function is used to approximate
233 the objective function. This surrogate function is represented by the Gaussian Processes in the
234 present study. The next optimal hyperparameters are found by this surrogate function. After that,
235 the surrogate function will be updated with the corresponding loss value. After repeating the
236 inference and updating process for a certain number of iterations, the most optimal
237 hyperparameters (x^*) can be finally determined (Wu et al., 2019).

$$238 \quad x^* = \arg \min_x f(x) \quad (2)$$

239 where, x is the hyperparameters of the ANN model; $f(x)$ is the loss value of the ANN model
240 applying on the test set; arg min is the objective function that aims to find the hyperparameters
241 x to make the function $f(x)$ minimum.

242

243 **2.4 k-folder cross validation**

244 k-folder cross validation is a statistical method that used for ANN model's performance
245 evaluation. The k-fold validation technique guarantees all samples in the dataset to be
246 considered for both training and validation processes. The process of k-fold cross validation is
247 illustrated in Fig. 3. The original dataset is randomly shuffled before the splitting. The shuffled
248 dataset is split into five folds. After that, each fold is sequentially treated as test set and the rest
249 folds are used to train the ANN model. For example, Fig. 3 shows the first cross validation
250 which uses the fold 1 data set as test set and the rest folds data as training set. In the present
251 study, the 5-folder cross validation is adopted. Therefore, the ANN model is trained and
252 evaluated five times.

253

254 **3. Data analysis and modelling results**

255 **3.1 Data distribution and correlation**

256 As discussed earlier, in the present study four influencing factors are used for the prediction

257 of volumetric UWC (θ_u) in frozen soils (i.e., the SSA, ρ_d , θ_{init} , and $Temp$). Table 2 summarizes
258 the statistical properties of the considered features and θ_u , including the mean, standard
259 deviation, minimum and maximum values. The preliminary data analysis shows the data range
260 of the collected data, which also provides a reference for the application range of the final
261 prediction model.

262 Figure 4 presents the histogram plots of the considered variables as well as the prediction
263 target. As can be seen from Fig. 4(a), most of the collected samples have a SSA lower than 200
264 m^2/g . However, there are a few samples whose SSA is larger than 600 m^2/g . The distribution of
265 initial volumetric water content is denser than that of SSA. Most samples' θ_{init} values are within
266 0.1 to 0.6 m^3/m^3 . The dry density value ranges from 0.26 to 1.93 g/cm^3 with a mean value at
267 1.41 g/cm^3 . Although the lowest temperature in the collected dataset is -64 °C, most samples
268 were tested in the temperature range of 0 to -30 °C. Only a few samples whose testing
269 temperature below -30 °C were collected. These samples are reserved in the model to fully
270 utilize the collected data. In the end, the final UWC of the collected samples ranges from 0.00
271 to 0.91 m^3/m^3 .

272 Figure 5 shows the correlation relationship among the input variables and the output. The
273 highest correlation among the input variables is between the dry density and initial volumetric
274 water content (-0.79), followed by the SSA (-0.62). However, well defined correlations were
275 not observed between any input variable and the volumetric UWC. This demonstrates that the
276 UWC prediction cannot rely on any single factor.

277

278 3.2 Bayesian optimization and training results

279 50 iterations were conducted for the Bayesian optimization as illustrated in Fig. 6. It
280 represents the optimization process that the ANN was trained multiple times with different
281 inferred hyperparameters. The objective of the optimization process is to increase the R -squared
282 value when predicting the samples' UWC in the test set. The R -squared value is defined in Eq.
283 (3). The closer of the predicted UWC to its measured counterpart, the higher R -squared value
284 would be.

$$285 \quad R^2 = 1 - \frac{SS_{res}}{SS_{tot}} \quad (3)$$

286 in which,

$$287 \quad SS_{res} = \sum_i (y_i - \hat{y}_i)^2 \quad (4)$$

$$288 \quad SS_{tot} = \sum_i (y_i - \bar{y})^2 \quad (5)$$

289 where, SS_{res} is the sum of squares of residual, and SS_{tot} is the sum of squares of the original
290 dataset; y_i is the measured UWC of each sample, and \bar{y} is the corresponding average value; \hat{y}_i
291 is the predicted UWC.

292 The R -squared value of the test set increased from around 0.61 to 0.82. In the end, an ANN
293 model with 64 batch size, 2 hidden layers with 128 neurons in each layer, and a learning rate at
294 0.004 was determined.

295 The optimal hyperparameters that obtained from Bayesian optimization were used to
296 determine the final ANN model. The model was then evaluated with the original dataset by
297 using 5-folder cross validation. The final performance of the ANN model at each fold can be
298 seen in Fig. 7(a) and one of the prediction results is shown in Fig. 7(b). The results indicate an
299 overall good performance of the ANN model, considering that the collected UWC data were
300 determined under different experimental scenarios. In particular, folders 1, 2 and 4 achieve a R -
301 squared value for the test set around 0.8. The average R -squared value among the five folders
302 is 0.76.

303

304 **3.3 Factor importance to the ANN model**

305 Although the ANN model performs well, it is often criticized as a ‘black box’ since it cannot
306 reveal the internal relationships among the input variables and prediction target. To solve this
307 issue, a ML model interpreter, the SHAP interpretation (Lundberg and Lee, 2017) is adopted
308 together with the LightGBM model trained with the balanced training dataset, to interpret the
309 contribution of each influencing factor. SHAP presents a way to calculate the additive feature
310 importance score for each factor (Strumbelj and Kononenko, 2010). The higher the importance
311 score, the more important is the factor towards the final ML model prediction. The SHAP
312 interpretation method together with decision-tree based ML algorithms have been widely used
313 in the civil engineering applications, including some scenarios where highly correlated

314 variables exist, such as the explanation of the failure of reinforced concrete (Mangalathu et al.,
315 2020) and the roadway segment crashes (Wen et al., 2021).

316 Figure 8 shows the overall importance of the influencing factors considered on the UWC.
317 It can be inferred that temperature has the largest impact, followed by the SSA. Furthermore,
318 the initial water content has the lowest influence on the final UWC. The specific individual
319 influence of each variable can also be analyzed by the adopted SHAP technique. As shown in
320 Fig. 9, a positive influence of temperature on the UWC can be observed. This means that the
321 UWC values are higher at higher temperature. Similar trends can also be observed for the SSA,
322 i.e., larger SSA is related to higher UWC. These are consistent with general observations.
323 However, the influence of dry density and initial water content is more controversial than other
324 variables, which indicates that their influence is also dependent on other variables.

325

326 **4. Comparison of the ANN model and two traditional models**

327 **4.1 Models description**

328 Many models for the estimation of the UWC in frozen soils have been proposed in the
329 literature. They can be generally classified into three types; namely, (i) empirical models, e.g.,
330 linear, power, and exponential relationships between UWC and subzero temperature and soil
331 physical properties; (ii) models that employ SWCC expressions to represent the relation
332 between UWC and subzero temperature, based on the similarity between frozen soils and
333 unsaturated soils; (iii) physical and theoretical models, which take advantage of soil
334 particle/pore size distribution, capillarity, adsorption, salt exclusion, and thermodynamic
335 theories. In the present study, two models from the first two categories are selected and
336 compared with the above developed ANN model. The physical and theoretical models are
337 complex for use. Therefore, no model from this category is selected for comparison.

338 The first model is empirical and was proposed by Anderson and Tice (1972). They
339 suggested that the UWC can be conveniently expressed as a function of subzero temperature
340 by a simple power curve with two constants, which can be estimated from soil SSA. This
341 empirical power relationship is one of the most widely used model in the literature. The model
342 is expressed in terms of volumetric UWC (θ_u) below,

$$\begin{cases} \ln w_u = 0.2618 + 0.5519 \ln SSA - 1.449 SSA^{-0.264} \ln(-T) \\ \theta_u = \rho_d w_u / 100 \end{cases} \quad (6)$$

where, w_u is the gravimetric UWC; T is the subzero temperature, °C; ρ_d is soil dry density, g/cm³.

The second model is based on the similarity between the SFCC and SWCC. This concept has been used in many studies (e.g., Nishimura et al., 2009; Liu and Yu, 2014; Ren et al., 2017; Teng et al., 2020). For example, Liu and Yu (2014) employed the Fredlund and Xing (1994) SWCC expression (Eq. (7)) to represent SFCC. The cryogenic suction in frozen soils is correlated with the subzero temperature through the Clapeyron equation, as shown in Eq. (8). In addition, there are many empirical relationships between the Fredlund and Xing model parameters (i.e., a , n , m , and ψ_{res}) and soil physical properties in the literature (e.g., Zapata et al., 2000; Witczak et al., 2006; Chin et al., 2010). For example, the relationships proposed by Zapata et al. (2000) are summarized in Table 3. Although these empirical relationships were developed on unsaturated soils, they are used to calculate the model parameters (a , n , m , and ψ_{res} in Eq. (7)) for frozen soils in the present study, assuming that there is exact similarity between unsaturated soils and frozen soils. After then, the volumetric UWC can be determined through Eq. (7),

$$\theta_u = \left[1 - \frac{\ln \left(1 + \frac{\psi_{cryo}}{\psi_{res}} \right)}{\ln \left(1 + \frac{10^6}{\psi_{res}} \right)} \right] * \left\{ \frac{\theta_{init}}{\left[\ln \left[\exp(1) + \left(\frac{\psi_{cryo}}{a} \right)^n \right] \right]^m} \right\} \quad (7)$$

$$\psi_{cryo} = -L\rho_w \ln \frac{T + 273.15}{T_0 + 273.15} \quad (8)$$

where, ψ_{cryo} is the cryogenic suction in kPa; ψ_{res} is the cryogenic suction at the residual state, kPa; θ_{init} is the initial volumetric UWC, m³/m³; L is the latent heat of fusion of water ($L = 334$ kJ/kg); ρ_w is the density of water ($\rho_w = 1000$ kg/m³); T_0 is the normal freezing temperature of water ($T_0 = 0$ °C). The calculated cryogenic suction versus subzero temperature relationship by Eq. (8) is approximately linear with a slope of about 1225 kPa/°C, when the subzero temperature is not too low (Ren, 2019).

For comparing the above two traditional UWC models with the developed ANN model in

367 the present study, four different types of soils were selected. It should be noted that the UWC
368 datasets of these four soils were not included in the training or validating process when
369 developing the ANN model. They are only used in the comparison of ANN prediction versus
370 traditional models. In other words, these four soils provide completely independent datasets for
371 comparing the three models, and therefore providing objective assessment of the model
372 performance. Among the four soils, three soils are plastic and the last soil is non-plastic. It
373 covers a variety of soil types, such as sand, silt, and high plastic bentonite. Their SSA is in a
374 wide range, with the minimum of 3 m²/g for fine sand and the maximum of 380.6 m²/g for
375 bentonite, as shown in Table 4. Therefore, the selected four soils are good representatives for
376 model comparison. In addition, the soil physical properties that are essential for employing the
377 three models are summarized in Table 4.

378

379 4.2 Comparison results

380 Figure 10 summarizes the prediction results by the two traditional models and the ANN
381 model on four different soils with significantly different physical properties. It can be seen that
382 the Fredlund and Xing (1994) model (with its parameters calculated by the empirical
383 relationships suggested by Zapata et al. (2000)) is not able to provide accurate estimation of the
384 UWC for these four soils. This approach typically overpredicts the UWC for plastic soils but
385 underestimates those for non-plastic soils. The Anderson and Tice (1972) model provides
386 reasonable predictions for silt; however, the estimations for the other three soils are poor. In
387 addition, this model results in unreasonably high UWC value when the subzero temperature is
388 close to 0 °C (see Fig. 10(c)). Meanwhile, the UWC values of the four soils predicted by the
389 ANN model are close to the measured data points, suggesting that the performance of the pre-
390 trained ANN model is good.

391 Figure 11 presents the comparison between the ANN model and the two traditional models;
392 the measured UWC values are plotted on the abscissa. This figure clearly shows that the UWC
393 values predicted by the two traditional models deviate from the 1:1 line, with most of the data
394 outside the ±15% absolute percentage error lines. In other words, the two models either over-
395 or under-estimate the UWC of the four soils. However, the prediction results by the ANN model
396 are closer to the 1:1 line, compared with the two traditional models. This suggests that the ANN

397 model outperforms the two traditional models, and has higher prediction accuracy.

398 For better illustration, the root mean squared error (RMSE) for the three models is shown
399 in Fig. 12. It clearly shows that the ANN model generally has much smaller RMSE values for
400 the four soils, compared with the other two models. The Anderson and Tice (1972) model
401 provides fair estimations for three types of soils but fails on the bentonite. The Fredlund and
402 Xing (1994) approach had the worst overall performance among the three models, which means
403 soil specific calibrations are crucial for the performance of this model.

404

405 **5. Discussion**

406 **5.1 Concerns regarding the ANN model development**

407 There are a variety of internal and external factors that influence the UWC in frozen soils.
408 Therefore, estimating UWC is ideally suited by ML models such as ANN, which is good at
409 learning the highly nonlinear relationships among complex factors. In the present study, an
410 ANN model was established and trained based on the UWC data collected from the literature.
411 The amount of UWC data used in this study, however, is still limited. This is because the
412 influencing factors that were considered in various published studies in the literature are
413 different and sometimes arbitrary. This limitation contributes to the discrepancies among the
414 collected data. Therefore, there is a need to set up large and reliable database for UWC, which
415 can facilitate the establishment of robust and widely applicable ML models for UWC estimation.

416 A search of more than 100 articles in the literature resulted in 20 articles (and 73 soils in
417 total) that contain the proper types of data. In order to obtain enough amount of data for
418 developing the ANN model, UWC data were selected regardless of the testing methods,
419 hysteresis effect, freeze-thaw cycles, or salt concentrations. This on one hand highlights the
420 versatility of the developed ANN model. On the other hand, ignoring hysteresis means that both
421 freezing and thawing UWC data were used. This partially contributes to prediction error. For
422 example, the data point (i.e., $0.181 \text{ m}^3/\text{m}^3$) in Fig. 10(b) is on the freezing branch, which is at
423 higher position than many other data points that are on the thawing branch. However, this
424 limitation can be alleviated if the experimental UWC data on freezing and thawing branches
425 are separately collected and used for establishing ANN models. Another issue that influences
426 the predicting accuracy of the developed ANN model is that the experimental data (used for

427 training and validation) themselves have some fluctuations or discrepancies. For example, the
428 discrepancy originated from the fact that different measurement techniques yield different
429 UWC values even for the same soil sample.

430 It is possible to use part of the data collected from the 20 articles, such that more
431 influencing factors (e.g., salinity and sand/silt/clay fraction) can be included to develop ANN
432 models. However, the present study limited its goal to use as much data as possible to ensure a
433 stable and reliable ANN model. A smaller range of data used for model development would also
434 limit its application scope and yield less reliable estimation results. In addition, [Pham et al.](#)
435 [\(2019\)](#) opined that including additional specific information to input features could affect
436 the representative capacity of the model because such information, in some cases, could not be
437 easily obtained in practice. The way to develop an ANN model with more influencing factors
438 essentially follows the same framework highlighted in the present study. Once more data are
439 available, the present ANN model can be easily extended in the future for improving its capacity
440 and performance.

441 [Géron \(2017\)](#) pointed out that in ANN modeling several hyperparameters, such as the
442 ANN structure, number of training steps and regularization coefficient, should be aligned.
443 Determining the most suitable combination of hyperparameters for a given task can be
444 challenging. The developed ANN model shows good performance on the test dataset. The
445 model performance may be further improved by developing ensemble or stacked models,
446 applying transfer learning, or performing domain knowledge modification ([Zhong et al., 2021](#)).
447 In addition, according to [Zhong et al. \(2021\)](#), the first step for developing a sound ANN model
448 is to build a large, consistent source dataset. Unfortunately, such a large dataset is currently not
449 available for the UWC data in the literature.

450 In the present study, four influencing factors (i.e., SSA, dry density, initial volumetric water
451 content and temperature) were employed as the input variables for estimating UWC. The SHAP
452 analysis shows that temperature and SSA are the two factors that significantly influence the
453 UWC in frozen soils, which is in agreement with general observations. It also indicates that the
454 initial water content does not have significant effect on UWC. In addition, the effect of density
455 (or void ratio) on UWC is not predominant, which is consistent with the study by [Wang et al.](#)
456 [\(2017b\)](#).

457

458 **5.2 The strengths and limitations of different models**

459 The [Anderson and Tice \(1972\)](#) model is empirical and simple. It uses the SSA and subzero
460 temperature as two independent variables for the calculation of UWC. Although this model was
461 established based on several soils with a variety of SSA values, it was not able to accurately
462 predict the UWC of three of the four selected soils. Therefore, this model should be further
463 improved using additional experimental data on different types of soils. It is likely a robust
464 correlation could be achieved between the UWC and SSA, and its parameters by including
465 additional experimental results. Another limitation of this model is that it yields a UWC value
466 of infinity when the subzero temperature approaches to 0 °C. This problem has also been
467 observed by other researchers (e.g., [Michalowski, 1993](#); [Qin et al., 2008](#)).

468 Using the [Fredlund and Xing \(1994\)](#) SWCC expression in the estimation of the UWC in
469 frozen soils is a semi-empirical approach and lacks theoretical foundation. This approach
470 employs the similarity between the SFCC and SWCC, and directly replaces the suction in
471 unsaturated soils by the cryogenic suction in frozen soils, which is calculated from subzero
472 temperature by using the Clapeyron equation. The validity of the Clapeyron equation generally
473 involves two assumptions; (i) thermodynamic equilibrium at the pore ice–water interface in the
474 frozen soil, and (ii) the pore ice pressure is equal to the atmospheric pressure. In spite that these
475 assumptions have been widely accepted as reasonable working hypotheses by many studies,
476 some aspects of the underlying theory have been recently disputed in the literature ([Vogel et al.,](#)
477 [2019](#); [Zhang et al., 2021a](#)). For example, it is likely that the thermodynamic process in freezing
478 soil is non-equilibrium, and pore ice pressure may deviate from the atmospheric pressure in
479 unsaturated frozen soil or when overburden pressure is present. More discussions related to the
480 similarity between freezing and drying processes are available in [Ren and Vanapalli \(2019\)](#). It
481 should also be noted that for this model, its parameters were determined based on empirical
482 relationships, which were derived from unsaturated soils. The failure of using this model in the
483 reliable prediction of UWC data suggests that the similarity and differences between the SFCC
484 and SWCC deserves more rigorous investigations.

485 [Mu \(2017\)](#) suggests that the empirical and SWCC-derived models may not provide reliable
486 UWC values over a wide temperature range due to lack of consideration of the influence of

487 both capillarity and adsorption. Furthermore, the effect of initial soil void ratio (which
488 influences the capillarity) on the UWC was not explicitly considered in these models. On the
489 other hand, the ANN model considered the effect of void ratio by incorporating the dry density
490 as an input variable. In addition, the empirical models lack a theoretical basis in terms of
491 continuum thermodynamics (Qin et al., 2008). Furthermore, although some of these models
492 have been successfully employed to best-fit the measured UWC data, they are not readily to be
493 used since the fitting parameters are generally based on a limited number of soils data. As a
494 result, it is not surprising that these fitting parameters cannot be used for estimating the UWC
495 of other soils such as the four types of soils analyzed in this study.

496 The comparison between the above two traditional models and developed ANN model
497 shows better performance of the latter. The ANN model has good applicability in frozen soils.
498 It can be applied to estimate the UWC of a variety of soils that were not employed for
499 developing the ANN model, and that of the soils used for training the model. However, one
500 limitation of the ANN model is that monotonic estimation of UWC cannot be guaranteed. For
501 example, it can be seen from Fig. 10(d) that a spike exists and the predicted UWC does not
502 strictly monotonically decrease with the decrement of temperature. The reason is that while
503 ANN model uses thousands of neurons to free from a fixed statistical model, there is no strict
504 equation to guarantee its output to be monotonic versus the temperature. Hence, the ANN model
505 predicts the UWC at each temperature separately. Making the ANN model realizing the
506 monotonicity in datasets requires more studies (Bandai and Ghezzehei, 2021).

507 The model from the third category (i.e., physical and theoretical model) was not selected
508 for comparisons. This is because such models generally involve several theories, assumptions,
509 parameters and approximations, resulting in inconvenient use of these models. Compared with
510 the macroscopic empirical and semi-empirical models from the first two categories, the physical
511 and theoretical models consider microscopic perspectives including in certain models at
512 molecular levels. For example, the theoretical model proposed by Watanabe and Mizoguchi
513 (2002) separately calculate the UWC in soil pores and that exists on particle surfaces as film
514 water. The former is based on pore size distribution and Gibbs-Thomson effect, and the latter
515 takes advantage of the specific surface area and thickness of the water film. The sum of the two
516 is the total UWC in the frozen soil. Similar concepts have been widely employed by recent

517 studies. However, as pointed by [Fisher et al. \(2019\)](#) that in order to use such models on natural
518 soils, detailed information of the soil properties is needed. They include such as the pore size
519 diameters and distribution, specific surface area, surface energy of the ice–water interface,
520 dielectric permittivity, and Hamaker constant, which would own multiple values since soil is a
521 complex and heterogeneous porous system ([Watanabe and Mizoguchi, 2002](#)). As a result, the
522 application of such models can be challenging.

523

524 **6. Summary**

525 The effects of climate change on the permafrost and seasonally frozen regions and the
526 increasing civil infrastructure construction in these regions have stimulated extensive research
527 studies related to the behaviors of frozen soils in recent years. It is well-known that unfrozen
528 water and pore ice coexist in the frozen soil as a result of complex soil-water interactions. The
529 relative quantity of the unfrozen water and ice has paramount influence on the physical and
530 mechanical properties of frozen soils, as well as on the transport of energy, water and solutes in
531 cold regions. Due to this reason, a variety of techniques have been developed and employed to
532 measure the unfrozen water and ice contents in frozen soils, and many models have also been
533 proposed for the estimation of UWC in the past several decades. These proposed models are
534 generally based on using soil physical properties, the similarity between frozen soils and
535 unsaturated soils, and / or physical and theoretical mechanisms.

536 Many factors influence the UWC in frozen soils. These factors include such as soil physical
537 and chemical properties, stress state, and temperature. The complex effects of these factors result
538 in a highly nonlinear relationship between these factors and UWC. In addition, the relative
539 contribution of each factor on UWC is not well-understood. Furthermore, the previously
540 developed statistical models generally can only incorporate a few influencing factors and
541 therefore have limited predicting capability. Such limitations, however, can be effectively
542 addressed by using ML algorithms, such as the ANN models.

543 In the present study, extensive UWC data of various types of soils tested under various
544 conditions were collected through a comprehensive search of the literature. An ANN model for
545 estimating the UWC in frozen soils was developed following the proposed modeling framework.
546 The ANN model was established by using the PyTorch package and its hyperparameters were

547 optimized with Bayesian optimization. The developed ANN model showed good performance
548 on the test dataset. In addition, it was compared with two traditional statistical models for UWC
549 prediction on four independent types of soils. The results indicated that the ANN model
550 achieved better UWC prediction performance than its counterparts, which include the empirical
551 model and semi-empirical model exploiting the similarity between frozen soils and unsaturated
552 soils. Detailed discussions on the developed ANN model, and the strengths and limitations of
553 different types of models were also presented. The present study demonstrates the potential of
554 ML model to provide reliable prediction of the UWC in frozen soils. In addition, the large
555 amount of UWC data collected and the developed ANN model will be great assets for future
556 studies.

557

558 **Acknowledgements**

559 The first author gratefully acknowledges the financial support from the Fundamental
560 Research Funds for the Central Universities (Izujbky-2021-kb03).

561

562 **References**

- 563 Akagawa, S., Iwahana, G., Watanabe, K., Chuvilin, E.M., Istomin, V.A. and Hinkel, K.M., 2012, June.
564 Improvement of pulse NMR technology for determination of unfrozen water content in frozen soils.
565 In Proceedings of the Tenth International Conference on Permafrost, Salekhard, Russia (Vol. 1, pp.
566 21-26).
- 567 Amankwah, S.K., Ireson, A.M., Maulé, C., Brannen, R., and Mathias, S.A., 2021. A Model for the Soil
568 Freezing Characteristic Curve That Represents the Dominant Role of Salt Exclusion. *Water*
569 *Resources Research*, 57(8), e2021WR030070.
- 570 Amiri, E.A., Craig, J.R. and Kurylyk, B.L., 2018. A theoretical extension of the soil freezing curve
571 paradigm. *Advances in Water Resources*, 111: 319-328.
- 572 Anderson, D.M. and Tice, A.R., 1972. Predicting unfrozen water contents in frozen soils from surface
573 area measurements. *Highway research record*, 393(2), pp.12-18.
- 574 Bai, R., Lai, Y., Zhang, M. and Yu, F., 2018. Theory and application of a novel soil freezing
575 characteristic curve. *Applied Thermal Engineering*, 129: 1106-1114.
- 576 Bandai, T., and Ghezzehei, T.A., 2021. Physics-informed neural networks with monotonicity constraints
577 for Richardson-Richards equation: Estimation of constitutive relationships and soil water flux
578 density from volumetric water content measurements. *Water Resources Research*, 57(2),
579 e2020WR027642.
- 580 Chai, M., Zhang, J., Zhang, H., Mu, Y., Sun, G. and Yin, Z., 2018. A method for calculating unfrozen
581 water content of silty clay with consideration of freezing point. *Applied Clay Science*, 161, pp.474-
582 481.

583 Chin, K. B., Leong, E. C., and Rahardjo, H., 2010. A simplified method to estimate the soil-water
584 characteristic curve. *Canadian Geotechnical Journal*, 47(12), 1382-1400.

585 Dillon, H.B. and Andersland, O.B., 1966. Predicting unfrozen water contents in frozen soils. *Canadian*
586 *geotechnical journal*, 3(2): 53-60.

587 Dongare, A.D., Kharde, R. R., and Kachare, A.D., 2012. Introduction to artificial neural network.
588 *International Journal of Engineering and Innovative Technology (IJEIT)*, 2(1), 189-194.

589 Ersahin, S., Gunal, H., Kutlu, T., Yetgin, B., and Coban, S., 2006. Estimating specific surface area and
590 cation exchange capacity in soils using fractal dimension of particle-size distribution. *Geoderma*,
591 136(3-4), 588-597.

592 Erzin, Y., Rao, B.H., and Singh, D.N., 2008. Artificial neural network models for predicting soil thermal
593 resistivity. *International Journal of Thermal Sciences*, 47(10), 1347-1358.

594 Fan, X., Zhang, X., and Yu, X.B., 2021. Machine learning model and strategy for fast and accurate
595 detection of leaks in water supply network. *Journal of Infrastructure Preservation and Resilience*,
596 2(1), 1-21.

597 Fisher, D. A., Lacelle, D., and Pollard, W., 2019. A model of unfrozen water content and its transport
598 in icy permafrost soils: effects on ground ice content and permafrost stability. *Permafrost and*
599 *Periglacial Processes*, 1-16.

600 Fredlund, D.G., and Xing, A., 1994. Equations for the soil-water characteristic curve. *Canadian*
601 *geotechnical journal*, 31(4), 521-532.

602 Géron, Aurélien, 2017. *Hands-on Machine Learning with Scikit-Learn & TensorFlow*.

603 Habibagahi, G., and Bamdad, A., 2003. A neural network framework for mechanical behavior of
604 unsaturated soils. *Canadian Geotechnical Journal*, 40(3), 684-693.

605 Head, T., G. L. MechCoder and I. Shcherbatyi, 2018. *scikit-optimize/scikit-optimize: v0. 5.2*. Zenodo.

606 Hu, G., Zhao, L., Zhu, X., Wu, X., Wu, T., Li, R., ... and Hao, J., 2020. Review of algorithms and
607 parameterizations to determine unfrozen water content in frozen soil. *Geoderma*, 368, 114277.

608 Ismeik, M. and Al-Rawi, O., 2014. Modeling soil specific surface area with artificial neural networks.
609 *Geotechnical Testing Journal*, 37(4), pp.678-688.

610 Jin, X., Yang, W., Gao, X., Zhao, J. Q., Li, Z., and Jiang, J., 2020. Modeling the unfrozen water content
611 of frozen soil based on the absorption effects of clay surfaces. *Water Resources Research*, 56(12),
612 e2020WR027482.

613 Kong, L., Wang, Y., Sun, W. and Qi, J., 2020. Influence of plasticity on unfrozen water content of frozen
614 soils as determined by nuclear magnetic resonance. *Cold Regions Science and Technology*, 172,
615 p.102993.

616 Kruse, A.M. and Darrow, M.M., 2017. Adsorbed cation effects on unfrozen water in fine-grained frozen
617 soil measured using pulsed nuclear magnetic resonance. *Cold Regions Science and Technology*,
618 142, pp.42-54.

619 Kurylyk, B. L., and Watanabe, K., 2013. The mathematical representation of freezing and thawing
620 processes in variably-saturated, non-deformable soils. *Advances in Water Resources*, 60, 160-177.

621 Lai, Y., Pei, W., Zhang, M., and Zhou, J., 2014. Study on theory model of hydro-thermal-mechanical
622 interaction process in saturated freezing silty soil. *International Journal of Heat and Mass Transfer*,
623 78, 805-819.

624 Lara, R.P., Berg, A.A., Warland, J., & Parkin, G., 2021. Implications of measurement metrics on soil
625 freezing curves: A simulation of freeze-thaw hysteresis. *Hydrological Processes*, 35(7), e14269.

626 Li, Z.M., Chen, J., and Sugimoto, M., 2020. Pulsed NMR Measurements of Unfrozen Water Content in
627 Partially Frozen Soil. *Journal of Cold Regions Engineering*, 34(3), 04020013.

628 Liu, Z. and Yu, X., 2013. Physically based equation for phase composition curve of frozen soils.
629 *Transportation Research Record: Journal of the Transportation Research Board*, (2349): 93-99.

630 Liu, Z. and Yu, X. 2014. Predicting the phase composition curve in frozen soils using index properties:
631 A physico-empirical approach. *Cold Regions Science and Technology*, 108: 10-17.

632 Lovell Jr, C.W., 1957. Temperature effects on phase composition and strength of partially-frozen soil.
633 *Highway Research Board Bulletin*, (168).

634 Lu, J., Pei, W., Zhang, X., Bi, J., and Zhao, T., 2019. Evaluation of calculation models for the unfrozen
635 water content of freezing soils. *Journal of Hydrology*, 575, 976-985.

636 Lu, N., Likos, W. J., Luo, S., and Oh, H., 2021. Is the Conventional Pore Water Pressure Concept
637 Adequate for Fine-Grained Soils in Geotechnical and Geoenvironmental Engineering?. *Journal of*
638 *Geotechnical and Geoenvironmental Engineering*, 147(10), 02521001.

639 Lundberg, S. and Lee, S.I., 2017. A unified approach to interpreting model predictions. arXiv preprint
640 arXiv:1705.07874.

641 Ma, T., Wei, C., Xia, X., Zhou, J. and Chen, P., 2015. Soil freezing and soil water retention
642 characteristics: Connection and solute effects. *Journal of performance of constructed facilities*,
643 31(1), p.D4015001.

644 Mangalathu, S., Hwang, S.H. and Jeon, J.S., 2020. Failure mode and effects analysis of RC members
645 based on machine-learning-based SHapley Additive exPlanations (SHAP) approach. *Engineering*
646 *Structures* 219: 110927.

647 Mao, Y., Romero Morales, E.E. and Gens Solé, A., 2018. Ice formation in unsaturated frozen soils. In
648 *Unsaturated Soils: UNSAT 2018: The 7th International Conference on Unsaturated Soils* (pp. 597-
649 602). The Hong Kong University of Science and Technology (HKUST).

650 McKenzie, J.M., Voss, C.I., and Siegel, D.I., 2007. Groundwater flow with energy transport and water-
651 ice phase change: numerical simulations, benchmarks, and application to freezing in peat bogs.
652 *Advances in water resources*, 30(4), 966-983.

653 Michalowski, R.L., 1993. A constitutive model of saturated soils for frost heave simulations. *Cold*
654 *regions science and technology*, 22(1), 47-63.

655 Ming, F., Li, D.Q., and Liu, Y.H., 2020. A predictive model of unfrozen water content including the
656 influence of pressure. *Permafrost and Periglacial Processes*, 31(1), 213-222.

657 Mu, Q.Y., 2017. Hydro-mechanical behaviour of loess at elevated and sub-zero temperatures. Doctoral
658 dissertation, The Hong Kong University of Science and Technology (HKUST), Hong Kong, China.

659 Mu, Q.Y., Ng, C.W.W., Zhou, C., Zhou, G.G.D. and Liao, H.J., 2018. A new model for capturing void
660 ratio-dependent unfrozen water characteristics curves. *Computers and Geotechnics*, 101, pp.95-99.

661 Nishimura, S., Gens, A., Olivella, S., and Jardine, R.J., 2009. THM-coupled finite element analysis of
662 frozen soil: formulation and application. *Géotechnique*, 59(3), 159-171.

663 Paszke, A., Gross, S., Chintala, S., Chanan, G., Yang, E., DeVito, Z., ... and Lerer, A., 2017. Automatic
664 differentiation in pytorch. 31st Conference on Neural Information Processing Systems (NIPS 2017),
665 Long Beach, CA, USA.

666 Pham, K., Kim, D., Yoon, Y., and Choi, H., 2019. Analysis of neural network based pedotransfer
667 function for predicting soil water characteristic curve. *Geoderma*, 351, 92-102.

668 Qin, Y.H., Zhang, J.M., Zheng, B., Qu, G.Z., 2008. The relationship between unfrozen water content
669 and temperature based on continuum thermodynamics. *Journal of Qingdao University: Engineering
670 and Technology*, 23(1), pp.77-82. (in Chinese)

671 Ren, J., 2019. Interpretation of the frozen soils behavior extending the mechanics of unsaturated soils.
672 Doctoral dissertation, University of Ottawa, Ottawa, Canada.

673 Ren, J., and Vanapalli, S.K., 2019. Comparison of soil-freezing and soil-water characteristic curves of
674 two Canadian soils. *Vadose Zone Journal*, 18(1), 1-14.

675 Ren, J., and Vanapalli, S.K., 2020. Effect of freeze–thaw cycling on the soil-freezing characteristic curve
676 of five Canadian soils. *Vadose Zone Journal*, 19(1), e20039.

677 Ren, J., Vanapalli, S. K., and Han, Z., 2017. Soil freezing process and different expressions for the soil-
678 freezing characteristic curve. *Sciences in Cold and Arid Regions*, 9(3), 221-228.

679 Ren, J., Vanapalli, S. K., Han, Z., Omenogor, K. O., and Bai, Y., 2019. The resilient moduli of five
680 Canadian soils under wetting and freeze-thaw conditions and their estimation by using an artificial
681 neural network model. *Cold Regions Science and Technology*, 168, 102894.

682 Ren, J., Zhang, S., Wang, C., Ishikawa, T. and Vanapalli, S.K., 2021. The Measurement of Unfrozen
683 Water Content and SFCC of a Coarse-Grained Volcanic Soil. *Journal of Testing and Evaluation*,
684 51(1).

685 Saberi, P.S. and Meschke, G., 2021. A hysteresis model for the unfrozen liquid content in freezing
686 porous media. *Computers and Geotechnics*, 134, p.104048.

687 Saha, S., Gu, F., Luo, X., and Lytton, R.L., 2018. Use of an artificial neural network approach for the
688 prediction of resilient modulus for unbound granular material. *Transportation Research Record*,
689 2672(52), 23-33.

690 Shahin, M.A., Jaksa, M. B., and Maier, H.R., 2001. Artificial neural network applications in
691 geotechnical engineering. *Australian geomechanics*, 36(1), 49-62.

692 Shahin, M.A., Jaksa, M. B., and Maier, H.R., 2008. State of the art of artificial neural networks in
693 geotechnical engineering. *Electronic Journal of Geotechnical Engineering*, 8(1), 1-26.

694 Shastri, A., 2014. Advanced coupled THM analysis in geomechanics. Doctoral dissertation, Texas
695 A&M University, College Station, USA.

696 Smith, M.W. and Tice, A.R., 1988. Measurement of the unfrozen water content of soils. comparison of
697 NMR (Nuclear Magnetic Resonance) and TDR (Time Domain Reflectometry) methods (No.
698 CRREL-88-18). COLD REGIONS RESEARCH AND ENGINEERING LAB HANOVER NH.

699 Strumbelj, E. and I. Kononenko, 2010. An efficient explanation of individual classifications using game
700 theory. *The Journal of Machine Learning Research* 11: 1-18.

701 Suzuki, S., 2004. Dependence of unfrozen water content in unsaturated frozen clay soil on initial soil
702 moisture content. *Soil science and plant nutrition*, 50(4), 603-606.

703 Teng, J., Kou, J., Yan, X., Zhang, S., and Sheng, D., 2020. Parameterization of soil freezing
704 characteristic curve for unsaturated soils. *Cold Regions Science and Technology*, 170, 102928.

705 Vogel, T., Dohnal, M., Votrubova, J., and Dusek, J., 2019. Soil water freezing model with non-iterative
706 energy balance accounting. *Journal of Hydrology*, 578, 124071.

707 Wang, C., Lai, Y. and Zhang, M., 2017a. Estimating soil freezing characteristic curve based on pore-
708 size distribution. *Applied Thermal Engineering*, 124: 1049-1060.

709 Wang, J., Nishimura, S., and Tokoro, T., 2017b. Laboratory study and interpretation of mechanical
710 behavior of frozen clay through state concept. *Soils and Foundations*, 57(2), 194-210.

711 Wang, M., Li, X., Liu, Z., Liu, J. and Chang, D., 2020a. Application of PIV Technique in Model Test
712 of Frost Heave of Unsaturated Soil. *Journal of Cold Regions Engineering*, 34(3), p.04020014.

713 Wang, M., Li, X., and Xu, X., 2021. An implicit Heat-Pulse-Probe method for measuring the soil ice
714 content. *Applied Thermal Engineering*, 117186.

715 Wang, Q., Liu, Y., Zhang, X., Fu, H., Lin, S., Song, S. and Niu, C., 2020b. Study on an AHP-entropy-
716 ANFIS model for the prediction of the unfrozen water content of sodium-bicarbonate-type
717 salinization frozen soil. *Mathematics*, 8(8), p.1209.

718 Watanabe, K. and Mizoguchi, M., 2002. Amount of unfrozen water in frozen porous media saturated
719 with solution. *Cold Regions Science and Technology*, 34(2), pp.103-110.

720 Watanabe, K. and Wake, T., 2009. Measurement of unfrozen water content and relative permittivity of
721 frozen unsaturated soil using NMR and TDR. *Cold Regions Science and Technology*, 59(1), pp.34-
722 41.

723 Wen, H., Bi, J., and Guo, D., 2020. Calculation of the thermal conductivities of fine-textured soils based
724 on multiple linear regression and artificial neural networks. *European Journal of Soil Science*, 71(4),
725 568-579.

726 Wen, X., Y. Xie, L. Wu and L. Jiang, 2021. Quantifying and comparing the effects of key risk factors
727 on various types of roadway segment crashes with LightGBM and SHAP. *Accident Analysis &
728 Prevention* 159: 106261.

729 Wen, Z., Ma, W., Feng, W., Deng, Y., Wang, D., Fan, Z., and Zhou, C., 2012. Experimental study on
730 unfrozen water content and soil matric potential of Qinghai-Tibetan silty clay. *Environmental earth
731 sciences*, 66(5), 1467-1476.

732 Wettlaufer, J.S., 1999. Ice surfaces: macroscopic effects of microscopic structure. *Philosophical
733 Transactions of the Royal Society of London. Series A: Mathematical, Physical and Engineering
734 Sciences*, 357(1763), 3403-3425.

735 Witzak, M., Zapata, C., Houston, W., 2006. Models incorporated into the current enhanced integrated
736 climatic model: NCHRP 9–23 project findings and additional changes after version 0.7. Final
737 Report, Project NCHRP.

738 Wu, J., Chen, X.Y., Zhang, H., Xiong, L.D., Lei, H. and Deng, S.H., 2019. Hyperparameter optimization
739 for machine learning models based on Bayesian optimization. *Journal of Electronic Science and
740 Technology* 17(1): 26-40.

741 Xiao, Z., Lai, Y., and Zhang, J., 2020. A thermodynamic model for calculating the unfrozen water
742 content of frozen soil. *Cold Regions Science and Technology*, 172, 103011.

743 Xu, X.Z., Oliphant, J.L. and Tice, A.R., 1985. Soil-water potential and unfrozen water content and
744 temperature. *Journal of Glaciology and Geocryology*, 7(1), pp. 1-14. (in Chinese)

745 Yoshikawa, K. and Overduin, P.P., 2005. Comparing unfrozen water content measurements of frozen
746 soil using recently developed commercial sensors. *Cold Regions Science and Technology*, 42(3),
747 pp.250-256.

748 Yu, F., Guo, P., Lai, Y., and Stolle, D., 2020a. Frost heave and thaw consolidation modelling. Part 1: A
749 water flux function for frost heaving. *Canadian Geotechnical Journal*, 57(10), 1581-1594.

750 Yu, F., Guo, P., Lai, Y., and Stolle, D., 2020b. Frost heave and thaw consolidation modelling. Part 2:
751 One-dimensional thermohydronechanical (THM) framework. *Canadian Geotechnical
752 Journal*, 57(10), 1595-1610.

753 Yukselen-Aksoy, Y. and Kaya, A., 2010. Method dependency of relationships between specific surface
754 area and soil physicochemical properties. *Applied Clay Science*, 50(2), pp.182-190.

755 Zapata, C.E., Houston, W.N., Houston, S.L., Walsh, K.D., 2000. Soil–water characteristic curve
756 variability. *Advances in Unsaturated Geotechnics*. American Society of Civil Engineers, pp. 84–
757 124.

758 Zhang, L., Zhuang, Q., Wen, Z., Zhang, P., Ma, W., Wu, Q., and Yun, H., 2021a. Spatial state
759 distribution and phase transition of non-uniform water in soils: Implications for engineering and
760 environmental sciences. *Advances in Colloid and Interface Science*, 102465.

761 Zhang, P., Yin, Z.Y., and Jin, Y.F., 2021b. State-of-the-art review of machine learning applications in
762 constitutive modeling of soils. *Archives of Computational Methods in Engineering*, 1-26.

763 Zhong, S., Zhang, K., Bagheri, M., Burken, J.G., Gu, A., Li, B., Ma, X., Marrone, B.L., Ren, Z.J.,
764 Schrier, J. and Shi, W., 2021. *Machine Learning: New Ideas and Tools in Environmental Science
765 and Engineering*. Environmental Science & Technology.

766 Zhou, J.Z., Meng, X., Wei, C., and Pei, W., 2020. Unified soil freezing characteristic for variably-
767 saturated saline soils. *Water Resources Research*, 56(7), e2019WR026648.

768 Zhou, J.Z., Tan, L., Wei, C.F. and Wei, H.Z., 2015. Experimental research on freezing temperature and
769 super-cooling temperature of soil. *Rock and Soil Mechanics*, 36(3), pp.777-785. (in Chinese)

770

List of Tables

Table 1. Unfrozen water content testing information from the literature

Table 2. Statistical properties of the collected data

Table 3. Correlations between the Fredlund and Xing model parameters and soil index properties

Table 4. The four soils selected for model comparison

Table 1. Unfrozen water content testing information from the literature

Data origin	No. of Soils	Internal factors (Soil main physical information)			External factors	SFCC branches	Testing methods	
		SSA	θ_{init}	ρ_d				
Smith and Tice (1988)	25	SSA	θ_{init}	ρ_d	/	T	Thawing	NMR, TDR
Suzuki (2004)	1	SSA	θ_{init}	ρ_d	Organic content, EC, Fraction	T	Thawing	NMR, TDR
Yoshikawa and Overduin (2005)	2	SSA	θ_{init}	ρ_d	/	T	Freezing	NMR, FDR, TDT
Watanabe and Wake (2009)	4	SSA	θ_{init}	ρ_d	Porosity, C_u , EC, Ignition loss	T	Thawing	NMR
Ma et al. (2015)	2	SSA	θ_{init}	ρ_d	LL, PL, Fraction	T	Thawing	NMR
Kruse and Darrow (2017)	6	SSA	θ_{init}	ρ_d	Cation treatment, CEC, PSD	T	Both	NMR
Wang et al. (2020a)	1	SSA	θ_{init}	ρ_d	LL, PL, Fraction	T	Thawing	NMR
Zhou et al. (2020)	1	SSA	θ_{init}	ρ_d	LL, PL, Fraction, Salinity	T	Thawing	NMR
Lovell (1957)	3	SSA*	θ_{init}	ρ_d	LL, PI, PSD	T	//	Calorimetry
Akagawa et al. (2012)	4	SSA*	θ_{init}	ρ_d	LL, PL, PI	T	Both	NMR
Wen et al. (2012)	1	SSA*	θ_{init}	ρ_d	LL, PL, Fraction	T	//	NMR
Zhou et al. (2015)	1	SSA*	θ_{init}	ρ_d	LL, PL, Fraction	T	Both	NMR
Mu (2017)	1	SSA*	θ_{init}	ρ_d	LL, PL, PI, Fraction	T , F-T, Stress state	Both	TDR
Chai et al. (2018)	1	SSA*	θ_{init}	ρ_d	LL, PL, PI, PSD, Salinity, pH	T	Thawing	NMR
Mao et al. (2018)	1	SSA*	θ_{init}	ρ_d	LL, PL, Porosity, Fraction	T	Freezing	EC measurement
Kong et al. (2020)	5	SSA*	θ_{init}	ρ_d	LL, PL, PI, Fraction	T	Freezing	NMR
Li et al. (2020)	3	SSA*	θ_{init}	ρ_d	PSD	T	Both	NMR
Ren and Vanapalli (2020)	5	SSA*	θ_{init}	ρ_d	LL, PL, PSD, Porosity	T , F-T	Both	FDR
Teng et al. (2020)	3	SSA*	θ_{init}	ρ_d	LL, PL, Fraction	T	Both	NMR
Wang et al. (2021)	3	SSA*	θ_{init}	ρ_d	LL, PL, PSD	T	Thawing	NMR

Note: SSA: Specific surface area; SSA*: Calculated SSA based on soil plasticity index (PI). The SSA values of a few soils are assumed, since their PI are not available; θ_{init} : Initial volumetric water content; ρ_d : Dry density (For the soil in Chai et al. (2018), its ρ_d value was obtained by personal communication); T : Temperature; EC: Electrical conductivity; Fraction: Sand/Silt/Clay fraction by weight; C_u : Uniformity coefficient; LL: Liquid limit; PL: Plastic limit; CEC: Cation exchange capacity; PSD: Particle size distribution curve; F-T: Freeze-thaw cycles; /: Not available; //: Unknow.

Table 2. Statistical properties of the collected data

Item	Unit	Mean	Std	Min	Max
SSA	m ² /g	91.33	145.00	0.90	714.00
θ_{init}	m ³ /m ³	0.39	0.16	0.07	0.83
ρ_d	g/cm ³	1.41	0.36	0.26	1.93
Temp	°C	-6.15	7.31	-64.00	0.00
θ_u	m ³ /m ³	0.12	0.11	0.00	0.91

Table 3. Correlations between the Fredlund and Xing model parameters and soil index properties

FX model parameter	Plastic soils ($PI > 0$)	Non-plastic soils ($PI = 0$)
a (kPa)	$a = 0.00364 * (wPI)^{3.35} + 4 * (wPI) + 11$	$a = 0.8627 * (D_{60})^{-0.751}$
n	$n = [-2.313 * (wPI)^{0.14} + 5] * m$	$n = 7.5$
m	$m = 0.0514 * (wPI)^{0.465} + 0.5$	$m = 0.1772 * \ln(D_{60}) + 0.7734$
ψ_{res} (kPa)	$\psi_{res} = 32.44 * \exp(0.0186 * (wPI)) * a$	$\psi_{res} = a / (D_{60} + 9.7 * \exp(-4))$
$wPI = P_{200} * PI$ where, P_{200} is the percentage passing the #200 U.S. standard sieve, as a decimal; PI is plasticity index, as a percentage; D_{60} is the particle size corresponding to 60% passing by weight, mm.		

Table 4. The four soils selected for model comparison

Soil ID	P_{200}	PI (%)	SSA (m²/g)	θ_{init} (m³/m³)	ρ_d (g/cm³)	Data origin
Silt	0.854	11.7	16.6	0.416	1.60	Zhou et al. (2020)
Loess	1	19.0	75.3	0.512	1.29	Mu (2017)
Bentonite	1	127.9	380.6	0.387	1.60	Kong et al. (2020)
Fine sand	0.23 [†]		3.0	0.331	1.57	Li et al. (2020)

[†]: This value is the D_{60} (Unit: mm).

List of Figures

Fig. 1. Framework for unfrozen water content prediction

Fig. 2. Structure of ANN model with input layer, hidden layer, and output layer

Fig. 3. Illustration of k-folder cross validation

Fig. 4. Histogram plot of the input variables and prediction target

Fig. 5. Correlation map among the input variables and prediction target

Fig. 6. Bayesian optimization process

Fig. 7. Results of ANN model

Fig. 8. Overall importance of the considered factors on the unfrozen water content

Fig. 9. Individual impact of the considered factors on the unfrozen water content

Fig. 10. Comparison between the ANN model and two traditional models

Fig. 11. Comparison of prediction accuracy of the ANN model and two traditional models

Fig. 12. The RMSE for the ANN model and two traditional models on four soils

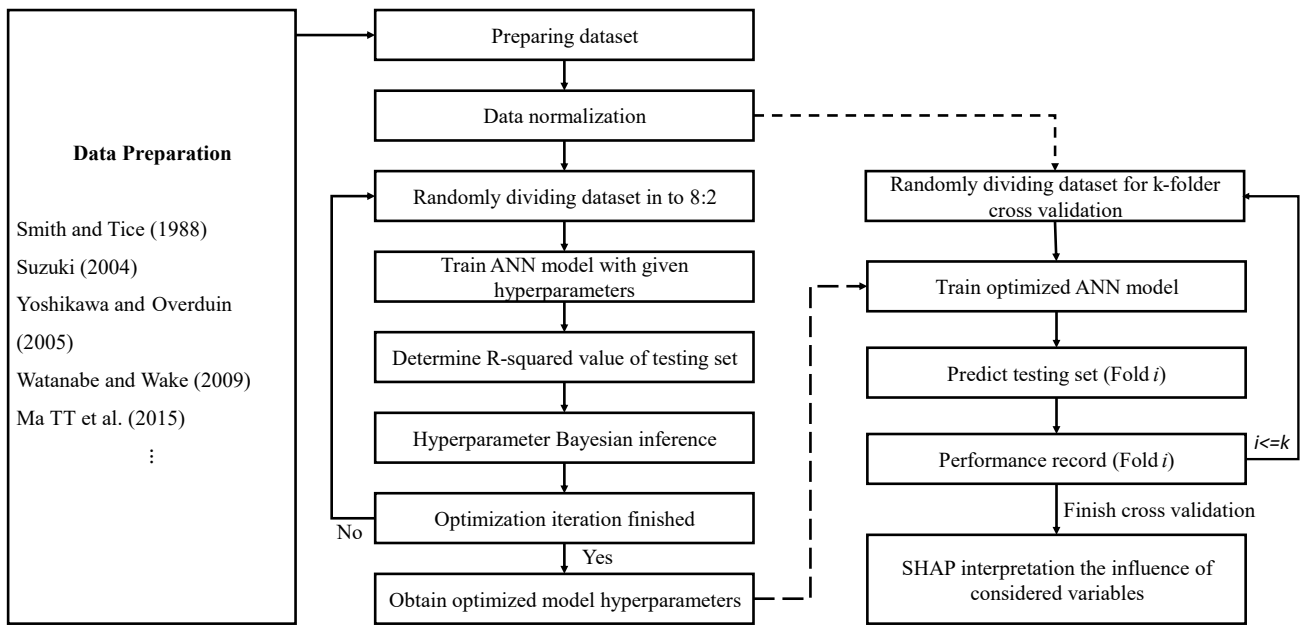


Fig. 1. Framework for unfrozen water content prediction

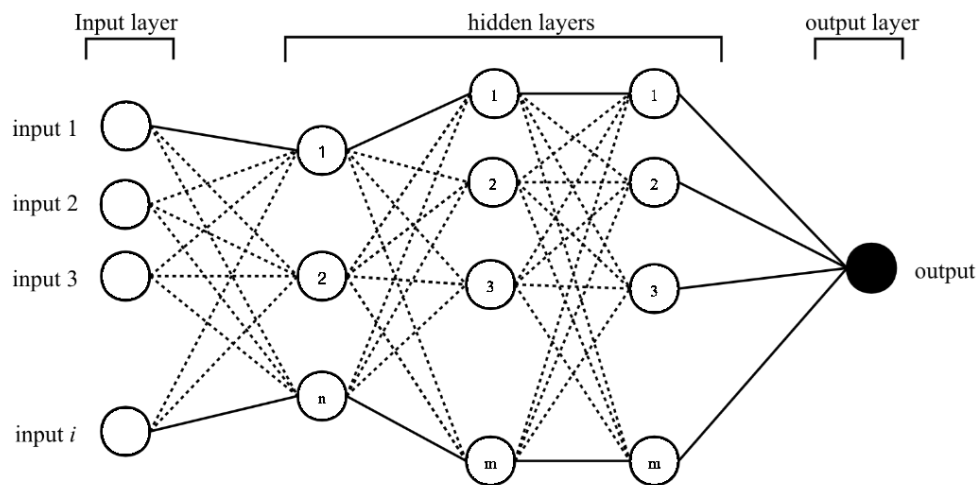


Fig. 2. Structure of ANN model with input layer, hidden layer, and output layer

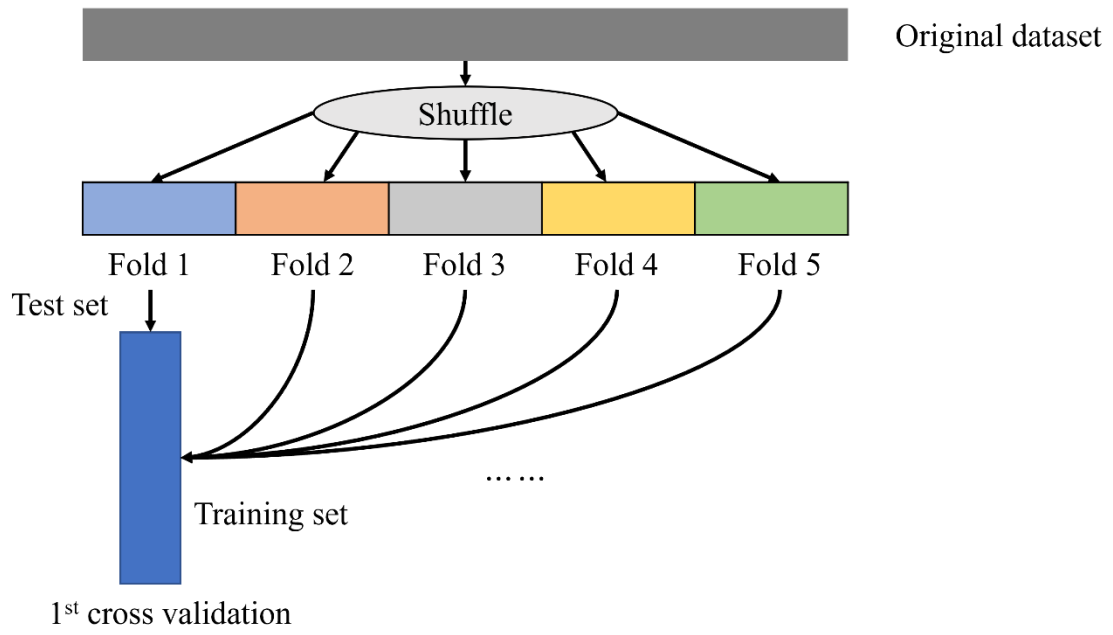
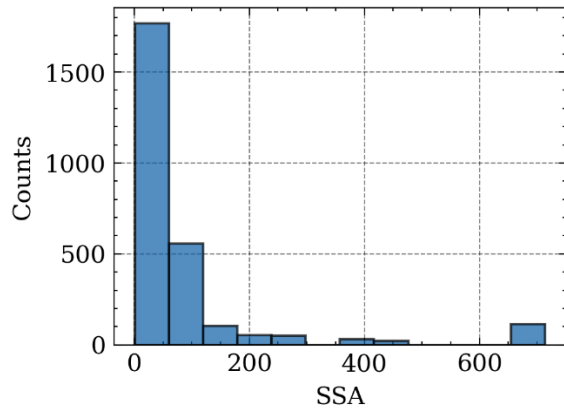
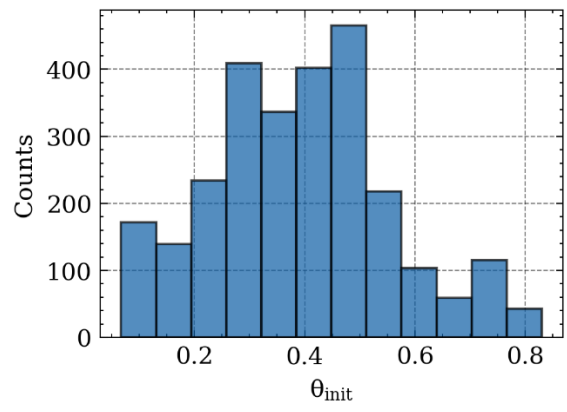


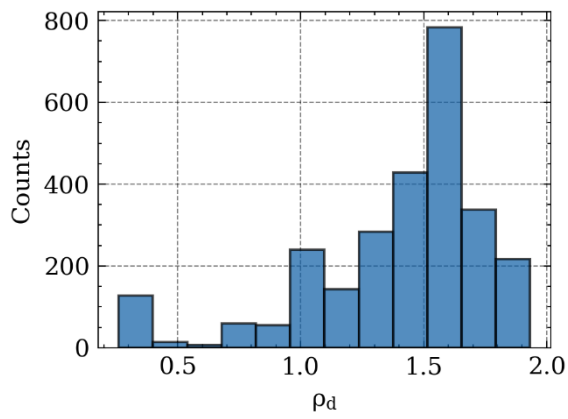
Fig. 3. Illustration of k-folder cross validation



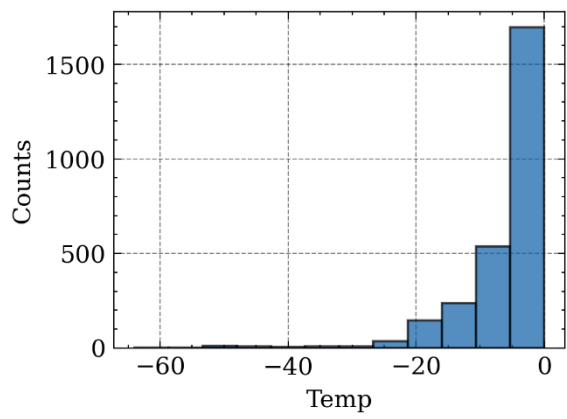
(a) Specific surface area



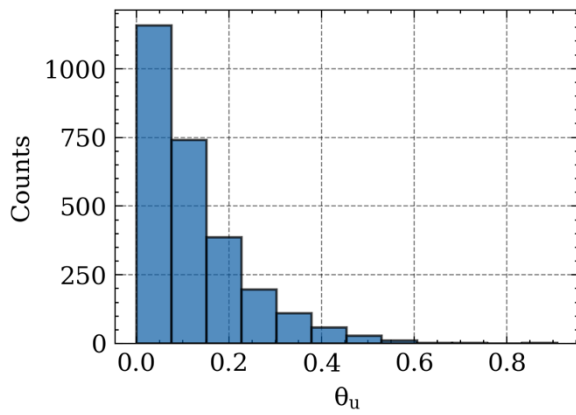
(b) Initial volumetric water content



(c) Dry density



(d) Temperature



(e) Unfrozen water content

Fig. 4. Histogram plot of the input variables and prediction target

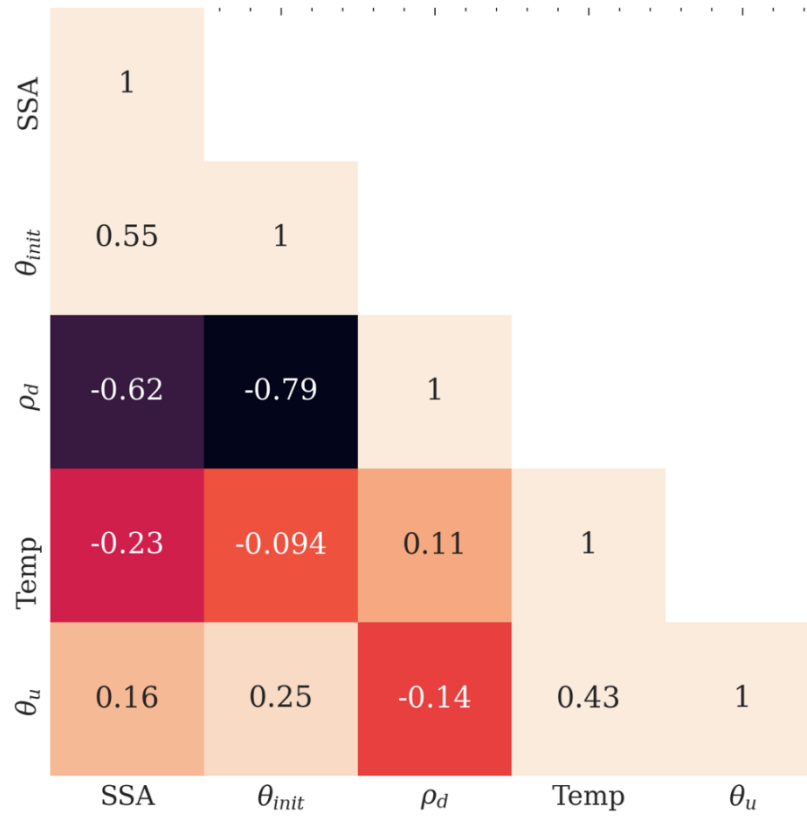


Fig. 5. Correlation map among the input variables and prediction target

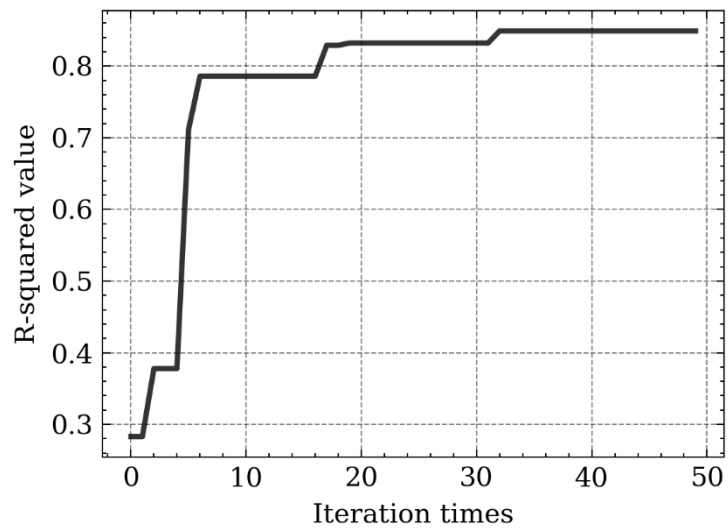
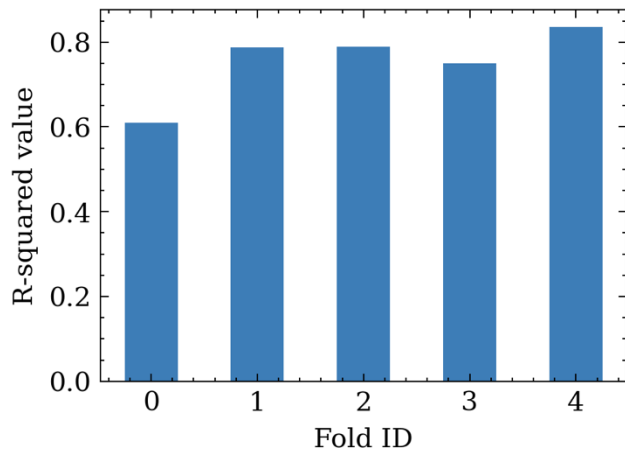
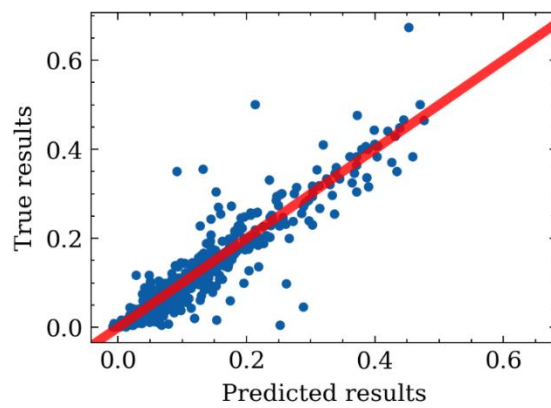


Fig. 6. Bayesian optimization process



(a) Prediction results of five folds



(b) Predicted water content in fold 2

Fig. 7. Results of ANN model

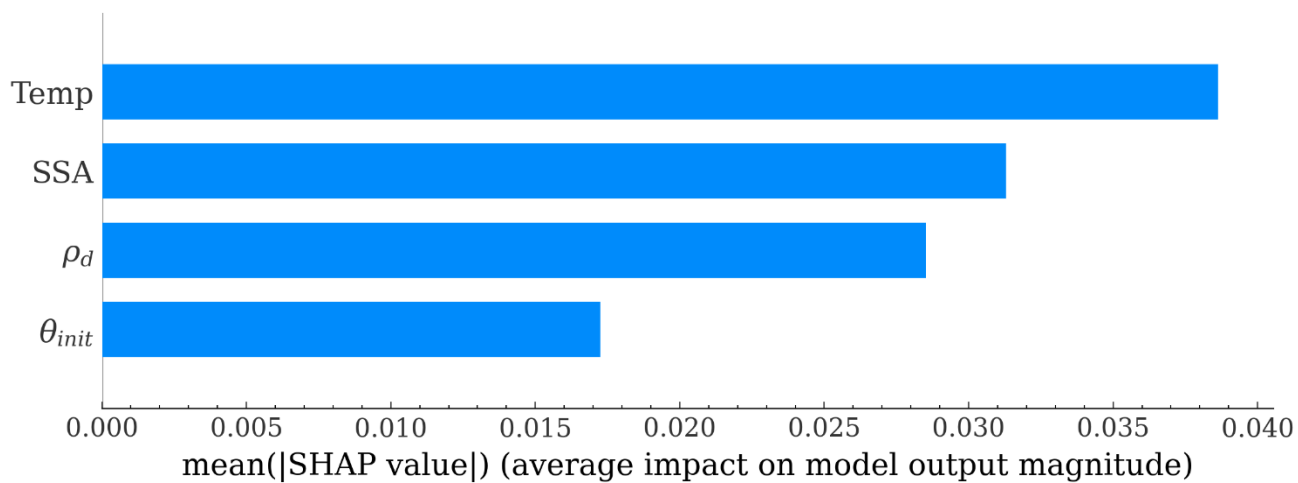


Fig. 8. Overall importance of the considered factors on the unfrozen water content

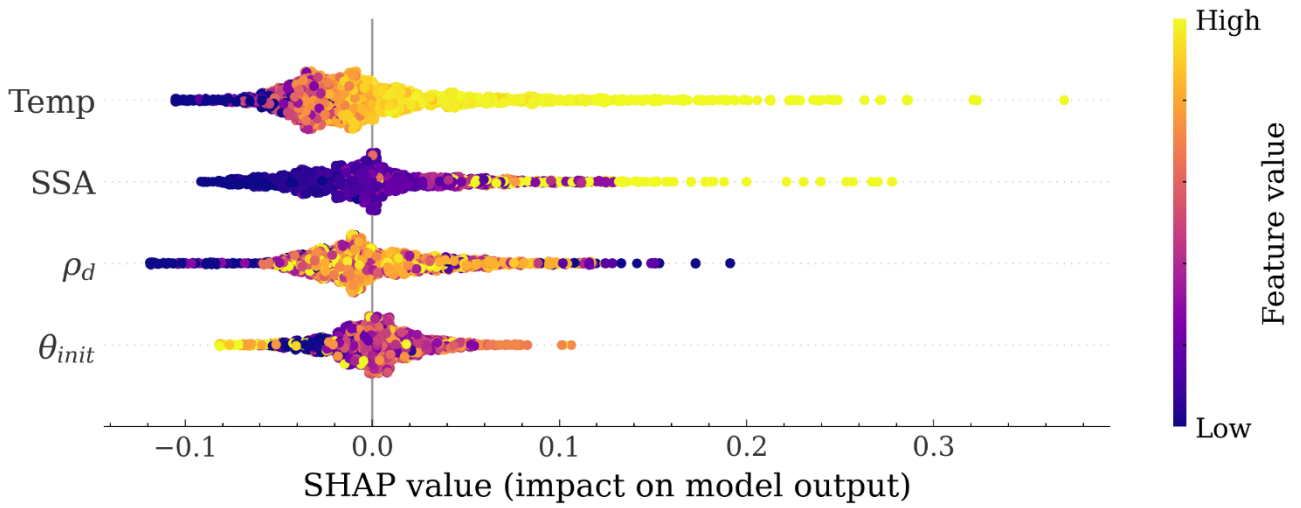


Fig. 9. Individual impact of the considered factors on the unfrozen water content

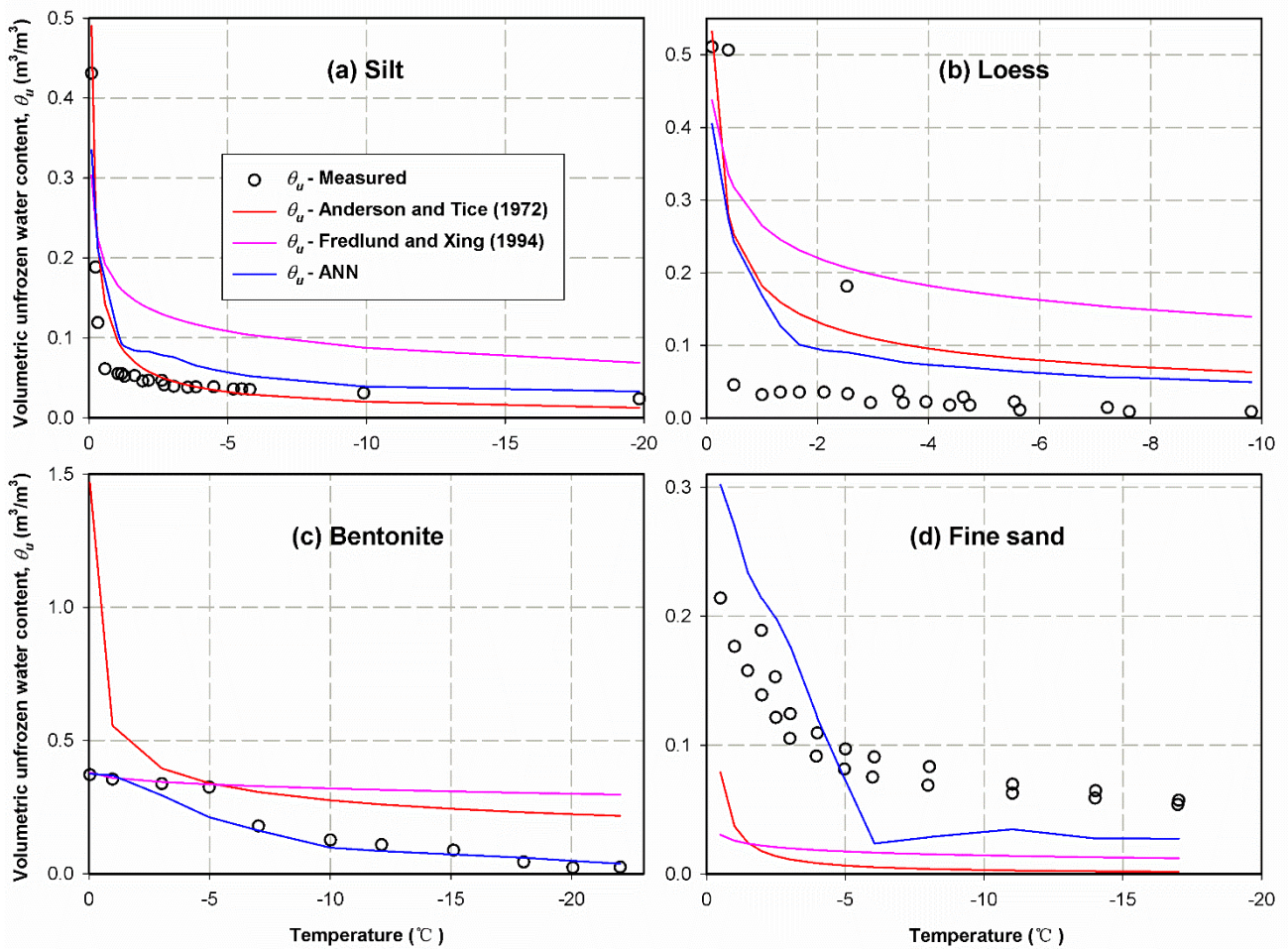


Fig. 10. Comparison between the ANN model and two traditional models

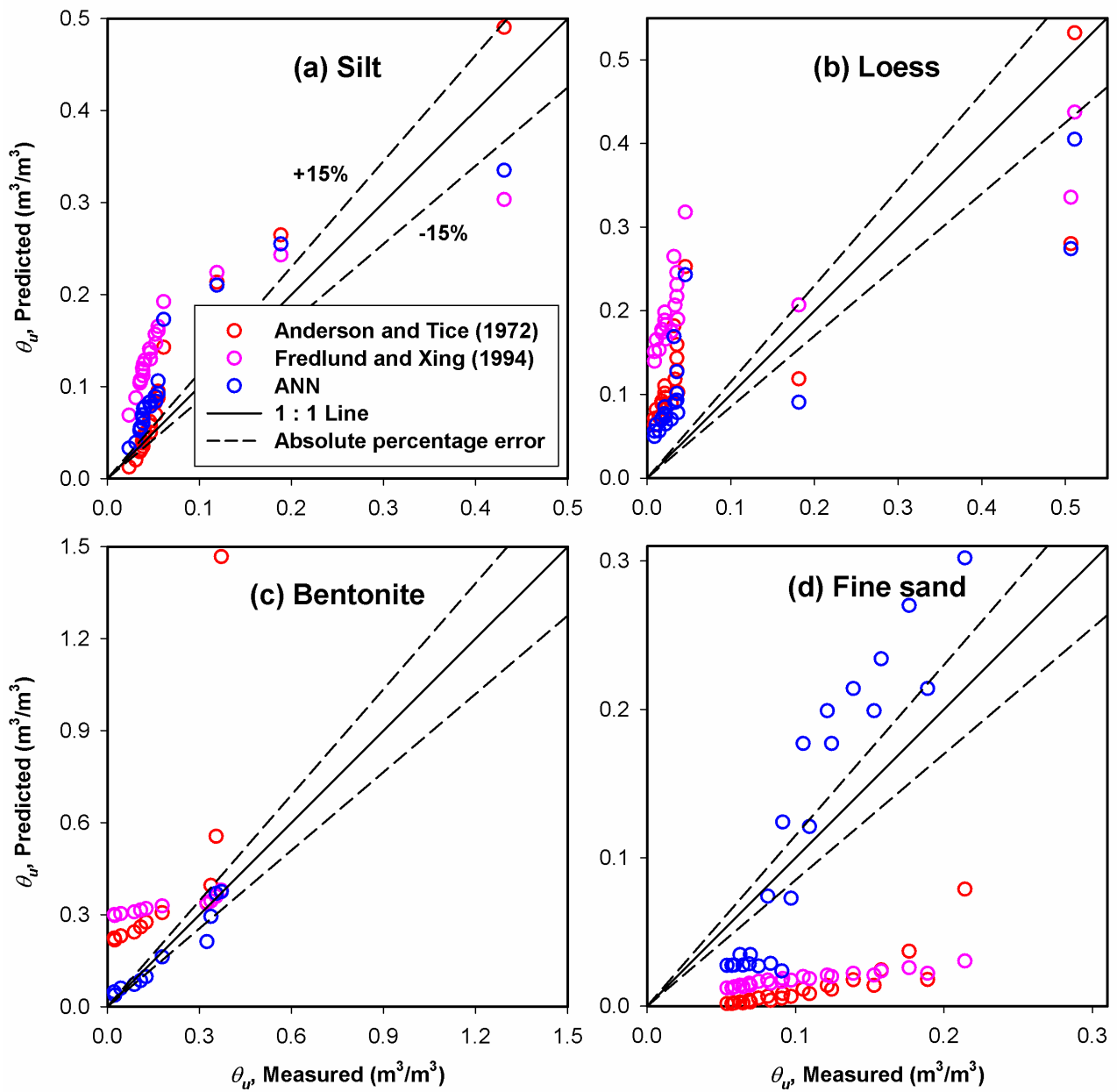


Fig. 11. Comparison of prediction accuracy of the ANN model and two traditional models

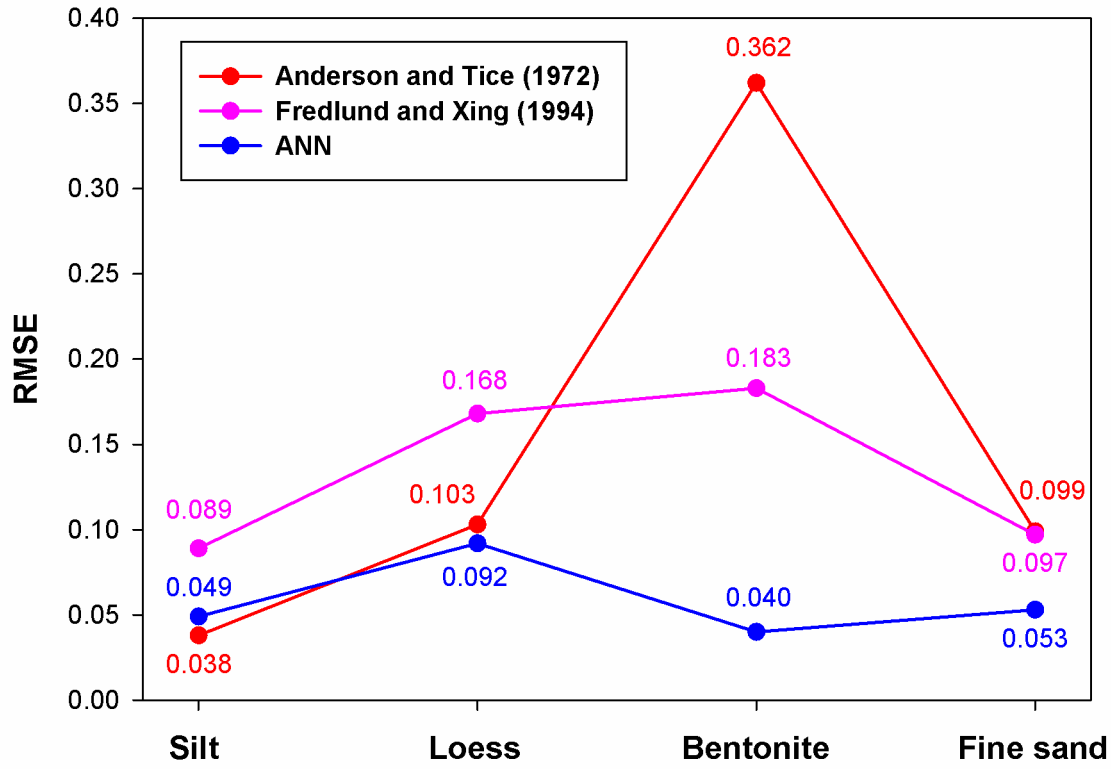


Fig. 12. The RMSE for the ANN model and two traditional models on four soils